Catal Lett (2008) 123:115–122
DOI 10.1007/s10562-008-9403-y

Transesterification of Dimethylcarbonate and Phenol Over Silica Supported TiO_2 and Ti-MCM 41 Catalysts: Structure Insensitivity

Upendra A. Joshi · Sun Hee Choi · Jum Suk Jang · Jae Sung Lee

Received: 26 November 2007 / Accepted: 9 January 2008 / Published online: 31 January 2008

Abstract Silica-supported titanium dioxide (TiO_2/SiO_2) and Ti-MCM 41 catalysts have been used for transesterification of dimethylcarbonate (DMC) and phenol to methylphenylcarbonate (MPC). The structure and the chemical state of titanium species in TiO_2/SiO_2 and Ti-MCM 41 have been investigated by means of X-ray diffraction (XRD), X-ray absorption near edge structure (XANES) for Ti K-edge and X-ray photoelectron spectroscopy (XPS). To understand the role of pore size on the activity of catalysts, different pore size silica supports (Q-series) were utilized in TiO_2/SiO_2 catalysts. Similarly, to understand the effect of Ti symmetry on the activity of catalysts, Ti-MCM 41 was used with different Ti-loadings. It was observed that the Ti surface area was an only important factor to achieve highest activity. In case of Ti-MCM 41 catalysts, as the Ti-loading increased octahedral symmetry increased and tetrahedral symmetry decreased. But, turnover rates based on the surface Ti atoms were independent of the Ti symmetry. They are also similar to those obtained for TiO_2/SiO_2 catalysts. Showing that transesterification of DMC and phenol over Ti-based catalysts is a structure insensitive reaction.

U. A. Joshi · J. S. Jang · J. S. Lee (✉)
Eco-friendly Catalysis and Energy Laboratory (NRL), Department of Chemical Engineering and School of Environmental Science and Engineering, Pohang University of Science and Technology (POSTECH), San 31, Hyojadong, Namgu, Pohang 790-784, Korea
e-mail: jlee@postech.ac.kr

S. H. Choi
Beamline Research Division, Pohang Accelerator Laboratory (PAL), Pohang University of Science and Technology (POSTECH), San 31, Hyojadong, Namgu, Pohang 790-784, Korea

Keywords Transesterification of dimethylcarbonate · Phenol · TiO_2/SiO_2 · Ti-MCM 41 · Linear combination of XANES · Structure insensitivity

1 Introduction

Polycarbonate is a widely used engineering plastic because of its excellent mechanical, optical, electrical and heat resistance properties. Conventionally it is produced by the interfacial polycondensation of bisphenol-A (BPA) and phosgene [1]. The major drawback of this conventional phosgene process is an environmental and safety problem involved in using copious amounts of methlyene chloride as the solvent and highly toxic phosgene as the reagent [2]. With increasing demands for safer and cleaner processes, the hazardous phosgene process has to be replaced by more environmentally friendly processes. The current phosgene-free process employs transesterification of diphenylcarbonate (DPC) with BPA. In 2002, about 12% of polycarbonate was produced by the phosgene-free technology. By 2007, this portion is expected to be greater than 20% [3].

Several alternative non-phosgene methods for the synthesis of DPC have been reported, including oxidative carbonylation of phenol and transesterification between phenol and dimethylcarbonate (DMC) [4, 5]. The oxidative carbonylation of phenol is not an effective method to produce DPC because of the use of noble metal catalysts and the low yield of DPC [6]. The transesterification of DMC and phenol takes place in two steps, as the direct synthesis of DPC (simultaneous reaction of 1 and 2 in the same reactor) is limited due to the low equilibrium constant for the forward reaction. Therefore DPC is obtained via two reactions of transesterification of DMC and phenol

(reaction 1) to give methylphenylcarbonate (MPC) followed by the disproportionation of formed MPC into DPC and DMC (reaction 2).

$$CH_3OH(C{=}O)OCH_3 + C_6H_5OH \rightleftharpoons C_6H_5O(C{=}O)OCH_3 + CH_3OH \quad (1)$$

$$2C_6H_5OH(C{=}O)OCH_3 \rightleftharpoons C_6H_5O(C{=}O)OC_6H_5 + CH_3O(C{=}O)OCH_3 \quad (2)$$

A variety of catalysts have been developed for the transesterification reaction of DMC and phenol to DPC, which include heterogeneous catalysts MoO_3/SiO_2 [7], PbO/MgO [8], lead and zinc double oxide [9], Mg–Al–hydrotalcite [10] and so on. Similarly, many homogeneous catalysts such as conventional Lewis acids [11], titanium esters [12], tin compounds [13] have been reported. We for the first time reported the TiO_2/SiO_2 catalysts for two step transesterification of DMC and phenol to DPC [14–16]. As there exists critical thermodynamic limitations for the synthesis of DPC from DMC and phenol especially in the reaction (1), much effort has been devoted to increasing the yield of MPC by employment of the complicated reactive distillation process. But it is desirable to devise a more improved catalytic system that could increase the yield of MPC from the reaction itself under modified reaction conditions, or by employing improved new catalysts as we did with the TiO_2/SiO_2 catalysts [14–16].

In this contribution we tried to find out the answers to the fundamental questions regarding the transesterification of DMC and phenol over Ti based heterogeneous catalysts, i.e., whether the pore size affects the catalytic reactivity or whether the rate of reaction depends upon the symmetry of titanium. Thus we carried out the transesterification reaction (1) over TiO_2/SiO_2 with different pore size silica as well as over Ti-MCM 41 with different Ti loadings. We also employed several spectroscopic techniques such as X-ray diffraction (XRD), X-ray photoelectron spectroscopy (XPS), X-ray absorption near edge structure (XANES), Barrett, Joyner and Halenda (BJH) pore size distribution and BET surface area in order to investigate the structure of active component and the correlation between the structure and the activity of the TiO_2/SiO_2 and Ti-MCM 41 catalysts.

2 Experimental

2.1 Catalysts Preparation

The SiO_2 samples with different pore sizes (CARiACT Q-15, Q-30 and Q-50 from Fuji Silysia Chemical Ltd. Japan) were impregnated with a solution of tetrabutoxytitanium (Aldrich 24411–2) dissolved in toluene. The resulting samples loaded with 10 wt% titanium (as Ti) were dried in an oven at 383 K for 12 h and then calcined in a quartz reactor at 773 K for 5 h with an air stream of 89 μmol s^{-1}. The final products are designated as TiO_2/SiO_2.

Ti-MCM 41 was synthesized with the procedure described elsewhere [17]. Template solutions $C_nH_{2n+1}(CH_3)_3$ NBr/OH were prepared by a partial ion exchange of $C_nH_{2n+1}(CH_3)_3NBr$ (Sigma) with Amberlite IRA-400 (OH) (Aldrich, 3 meq g^{-1} of template). Tetraethylorthosilicate and tetrabutylorthotitanate were dissolved into the solution and the mixture was stirred for 0.5 h. Zeosil amorphous silica, (Hanbul Chemicals) was added to give a template/Si mole ratio of 0.5 and varying Si/Ti ratios and the mixture was stirred for another 0.5 h. The resulting solution was heated without stirring at 393 K for three days. Solid products were recovered by filtration, washed with water and then dried in an oven at 333 K for a day. The synthesized samples were calcined at 813 K in helium for 2 h and then in oxygen for 6 h to remove the organic template from the pores of Ti-MCM 41.

2.2 Liquid Phase Transesterification of DMC and Phenol

The liquid phase transesterification of DMC and phenol was carried out in a 300 cm^3 autoclave (Parr) reactor. The 2 g of catalysts were charged along with a mixture of DMC (714.0 mmol) and phenol (142.8 mmol) into the reactor. While stirred, the reactor was flushed with nitrogen gas several times and pressurized with nitrogen gas (initial pressure 6.8 atm of N_2 at 293 K). The reactor was heated to the reaction temperature at a rate of 10.8 K min^{-1}. When temperature reached 433 K, it was assumed to be the start of reaction. Sampling was performed every hour by using two sampling valves attached on the sampling loop. The liquid products were filtered into a microsyringe and analyzed by using HP 5890II gas chromatograph (GC) equipped with a flame ionization detector (FID).

2.3 Characterization of the TiO_2/SiO_2 and Ti-MCM 41 Catalysts

The specific surface areas of the catalysts were determined on a constant volume adsorption apparatus (Micrometrics ASAP 2021C surface area analyzer) by the N_2 BET method at the liquid nitrogen temperature. Powder X-ray diffraction (XRD) measurements were conducted on an X-ray diffractometer of model M18XHF of MAC Science Co. using a radiation source of Cu Kα ($\lambda = 1.5405$ Å) at 40 kV and 200 mA with a scanning rate of 4° min^{-1}.

X-ray photoelectron spectroscopy (XPS) measurements were carried out using a Perkin-Elmer PHI 5400ESCA spectrometer with monochromatic Mg Kα radiation (1253.6 eV) at 15 kV and 20 mA. The vacuum in the measurement chamber, during the collection of spectra, was maintained below 5×10^{-9} torr. The pass energy of the measurement was 89.45 eV. The charging effect was circumvented by referencing binding energies to that of C_{1S} peak at 284.6 eV. X-ray absorption near edge structure (XANES) spectra were taken of the *K*-edge of Ti in a transmission mode at the beamline 3C1 of Pohang Accelerator Laboratory (PAL) in Korea, operating at 2.5 GeV with ca. 130–180 mA of the stored current. The radiation was monochromatized using a Si(111) double-crystal monochromator. The incident beam to samples was detuned by 30% in order to minimize the higher order reflections of the silicon crystals. The intensities of the incident and transmitted beams were monitored using separate ionization chambers, through which flowed pure N_2. The obtained data were analyzed with the IFEFFIT suite software programs [18]. The edge energy E_0 was defined as the inflection point in the rising portion of absorption feature. The preedge background was removed by using a simple linear fit. The resulting spectrum was then normalized by using the absorbance at E_0, which was extrapolated to E_0 after calculating a postedge background function with a quadratic polynomial in the region between of $E_0 + 150\ eV$ and $E_0 + 600$ eV.

3 Results

3.1 Liquid Phase Transesterification of DMC and Phenol Over TiO_2/SiO_2 and Ti-MCM41 Catalysts

As we already screened different catalysts and found that the TiO_2/SiO_2 performed better than other catalysts [14], TiO_2 supported on silica catalysts was utilized in this study of the transesterification of DMC and phenol. The silica support having different pore sizes has been utilized to investigate the effect of pore size distribution on the activity of the catalysts. The silica supports, namely, Davisil, Q-15, Q-30, Q-50 have pore sizes of 15 nm, 20 nm, 27 nm and 38 nm respectively. As we already optimized the titanium concentration in our previous work, the titanium was impregnated on these supports with 10 wt% loading. Phenol conversion and selectivity to MPC was determined at a time on stream of *ca.* 10 h when a steady state reaction was established. The MPC selectivity (%) is defined as the moles of MPC produced per 100 mole of phenol consumed.

Table 1 presents the activity of liquid phase transesterification of DMC and phenol to MPC. The specific surface area of catalysts was calculated by the BET method. The surface concentration of different component was obtained from XPS analysis. It is observed that the surface concentration of Ti is almost the same although the surface area decreases. Phenol conversion is higher in case of Davisil silica support catalysts compared to Q-series. Furthermore selectivity is almost constant in all catalysts. The turnover rate of MPC formation was calculated by considering surface atom density of TiO_2 (3.7 μmol/m^2). Except of the silica supported catalysts, the turnover rate remains almost same.

To understand the effect of titanium symmetry on the catalytic activity of transesterification of DMC and phenol, we prepared Ti-MCM 41 catalysts with different Ti loadings. The results of transesterification reaction are shown in Table 2. As the titanium loading increases, the titanium surface concentration increases and so does the phenol conversion. Overall the MPC selectivity based on DMC was more than 99% at the study state in all cases. The turnover rates showed slight increase with Ti steady loading, but the maximum variation was only 22%.

3.2 X-ray Diffraction Analysis

The crystalline phases of prepared catalysts were determined by X-ray diffraction. Figure 1a shows the XRD patterns of

Table 1 Liquid phase transesterification of DMC and phenol to MPC: Catalytic activity with 10 wt% TiO_2 supported on different silicas[a]

Support	Specific surface area of catalyst (m^2/g)	Specific surface area of support (m^2/g)	Average pore diameter (nm)[b]	Surface concentration (at %)[c]			TiO_2 surface area (specific surface area × TiO_2 conc) /100 (m^2/g)	Phenol conversion (%)	MPC selectivity (%)	Turnover rate of MPC (s^{-1}) × 10^{-3}
				Ti	Si	O				
Davisil	271.7	267.6	15	1.9	23.7	74.2	5.3	7.5	99.7	0.34
Q-15	191.8	188.6	20	2.1	23.9	73.9	4.0	6.2	99.5	0.41
Q-30	127.3	121.2	27	2.3	25.0	72.5	2.9	5.5	99.6	0.32
Q-50	86.5	72.0	38	2.2	28.8	73.1	1.9	4.2	99.3	0.19

[a] Reaction condition: Charge of DMC = 714.0 mmol, Charge of phenol = 142.8 mmol, Catalyst loading = 2.0 g, Stirring rate = 700 rpm, initial pressure = 6.8 atm of N_2 at 293 K, reaction temperature = 433 K

[b] By BJH pore size distribution

[c] By XPS

Table 2 Liquid phase transesterification of DMC and phenol to MPC: Catalytic activity over Ti-MCM 41 with different Si/Ti ratio[a]

Catalysts (Si/Ti ratio)	Specific surface area of catalyst (m^2/g)	Surface concentration (at %)[b]			TiO_2 surface area (specific surface area × TiO_2 Conc)/100 (m^2/g)	Phenol conversion (%)	MPC selectivity (%)	Turnover rate of MPC (s^{-1}) × 10^{-3}
		Ti	Si	O				
100	1165	0.34	25.1	74.2	3.96	5.56	99.3	0.53
60	1147	0.43	24.9	73.9	4.93	7.75	99.5	0.63
39	1100	0.45	25.0	74.1	4.95	9.02	99.6	0.78
24	1101	0.47	24.8	74.2	5.17	9.72	99.4	0.86
17	1105	0.50	25.2	73.8	5.52	10.52	99.6	0.94
12	1063	0.94	25.0	74.2	9.99	11.63	99.5	1.06
9	1122	1.16	25.2	73.9	12.9	12.54	99.7	1.18

[a] Reaction condition: Charge of DMC = 714.0 mmol, Charge of phenol = 142.8 mmol, catalyst loading = 2 g, stirring rate = 700 rpm, initial pressure = 6.8 atm of N_2 at 293 K, reaction temperature = 433 K

[b] By XPS

TiO_2/SiO_2 catalysts with different pore size silica. Weak but characteristic peaks of anatase type TiO_2 were detected as marked in all samples. Note that the loading of titanium is the same (10 wt%) for all samples. Thus, we observe exactly the same pattern for all samples irrespective of the supports of different surface area and pore size. Figure 1b shows the small angle-XRD patterns of Ti-MCM 41 having different Si/Ti ratios. The peaks could be indexed as *hko* reflections of a hexagonal lattice. This diffraction pattern is originated from the regular hexagonal array of uniform channels, characteristics of MCM 41. The position of the first (100) peak gives the repetition distance of the pores d_{100} by the Braggs law or the lattice parameter a of the hexagonal unit cell by $a = 2d_{100}/\sqrt{3}$. As the Ti concentration is increased in the system, there is a gradual shift of (100) peak to lower 2θ positions. This may reflect the fact that the preferred Ti–O–Si distance (0.36 nm) is larger than that of Si–O–Si (0.34 nm). Introduction of more Ti also reduces the regularity of pore structure as indicated by the reduced XRD peak intensity. This again appears to be due to the different preferred distance between Ti–O–Ti and Si–O–Si. This introduction of Ti into the Si framework would disturb the regularity of silicate framework. It is important to note that at the highest Ti concentration (Si/Ti = 9) the sample has lost the most of the intensity of the second and third XRD peaks characteristics of Ti-MCM 41 structure as shown in Fig. 1b.

3.3 Linear Combination of XANES

In XANES ranging from *ca.* 20 eV below an absorption edge to *ca.* 100 eV above it, an electron at a core level is photo-excited to the unoccupied level above the Fermi level. Thus the features in XANES give information about the local structures such as formal valence of an absorbing element, its coordination environment, and subtle geometrical distortions. The coordination state of Ti in titanium oxides has often been probed by Ti *K*-edge XANES in a qualitative manner by comparison of shape or intensity of preedge peak with XANES spectra of reference materials. In the

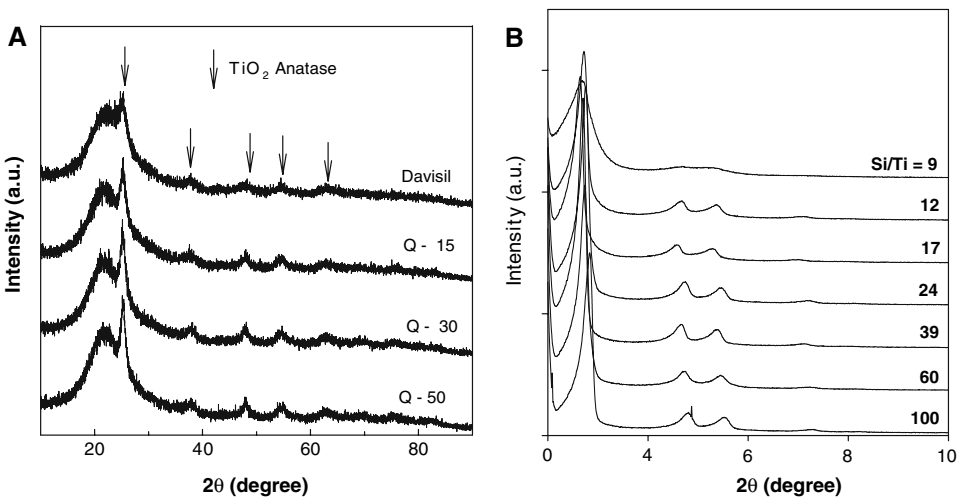

Fig. 1 X-ray diffraction pattern of (**a**) TiO_2/SiO_2 with different silica, (**b**) Ti-MCM 41 with different Si/Ti ratio

tetrahedral symmetry of Ti(IV), a strong single peak is experimentally observed in the preedge region due to allowed A_1-into-E_1 transition. However, octahedral Ti(V) are characterized by three weak peaks of which two come from the forbidden transitions of A_{1g}-into-T_{2g} and E_g and the third peak at the lowest energy is of uncertain origin [19, 20]. Titanium oxides with anatase and rutile structures show three weak pre-edge peaks, indicating an octahedral symmetry of Ti cation surrounded by six O anions.

Figures 2 and 3 show the XANES spectra of TiO_2/SiO_2 and Ti-MCM 41 respectively. In case of TiO_2/SiO_2 catalysts of the same Ti loading, no difference was observed in the preedge peak intensity and its shape. In Fig. 3, attention was focused on the changes in preedge peak intensity as the amount of Ti was increased. As the amount of Ti increases, the pure Ti–O–Si network having tetrahedral symmetry of Ti was gradually replaced with Ti–O–Ti octahedral symmetry (from Si/Ti = 24–9). The shoulder peak in these samples implies formation of some Ti–O–Ti bonds having octahedral symmetry of Ti.

Our objective in this study is the quantification of two different Ti species in Ti–O–Si and Ti–O–Ti bonding by using the linear combination of two references XANES spectra and correlated them with the catalytic activity. To do so, preliminary consideration must be made on the reference

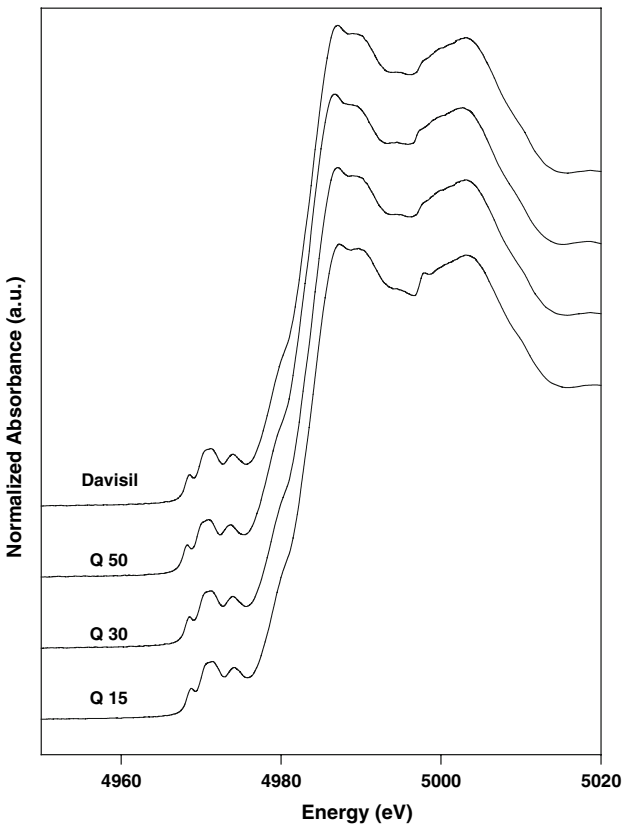

Fig. 2 Ti K-edge XANES spectra of TiO_2/SiO_2 with different silica

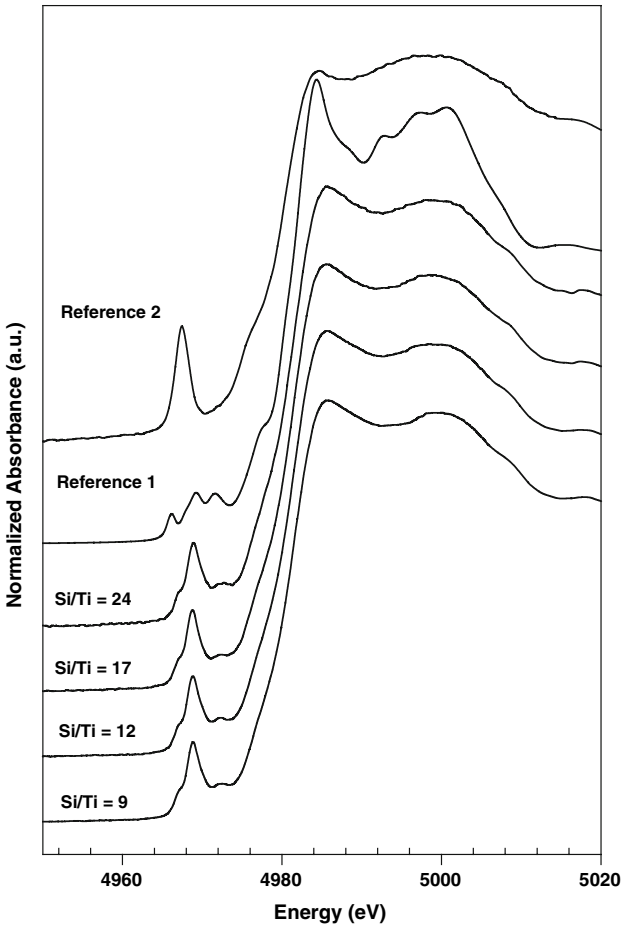

Fig. 3 Ti K-edge XANES spectra of Ti-MCM 41 with Si/Ti = 9–24, Reference 1 is anatase and Reference 2 is Ti/Si = 0.04 from [19]

spectra. One is the anatase type TiO_2, which contains pure Ti–O–Ti bonds with the octahedral symmetry of Ti cation surrounded by six O anions. Furthermore the XRD patterns of high Ti loading samples indicated the presence of anatase TiO_2 crystallites and postedge XANES features matched only those of anatase but not those of rutile. Thus, anatase is the natural choice as a reference for Ti–O–Ti bonds. Another one is the titanium–silicon mixed oxide with Ti/Si = 0.04 made from sol-gel method reported previously [20–22]. Actually we also prepared Ti-MCM-41 with Si/Ti = 39, 60, and 100 and compared their preedge peak intensity with that of our previous material $(Ti_xSi_{1-x})O_2$ with Si/Ti = 25. As shown in Fig. 4, the preedge peak intensity did not increase as the Ti loading decreases to the low levels. This is probably due to the formation of a small number of octahedral holes when tiny amount of TiO_2 is introduced to SiO_2 matrix [20, 23, 24]. Therefore we adopted the $(Ti_xSi_{1-x})O_2$ with Ti/Si = 0.04 as for the reference containing the maximum Ti–O–Si with Ti cations surrounded by four O anions in tetrahedral symmetry without any indication of the presence of Ti–O–Ti bonding. The validity of the choice of these

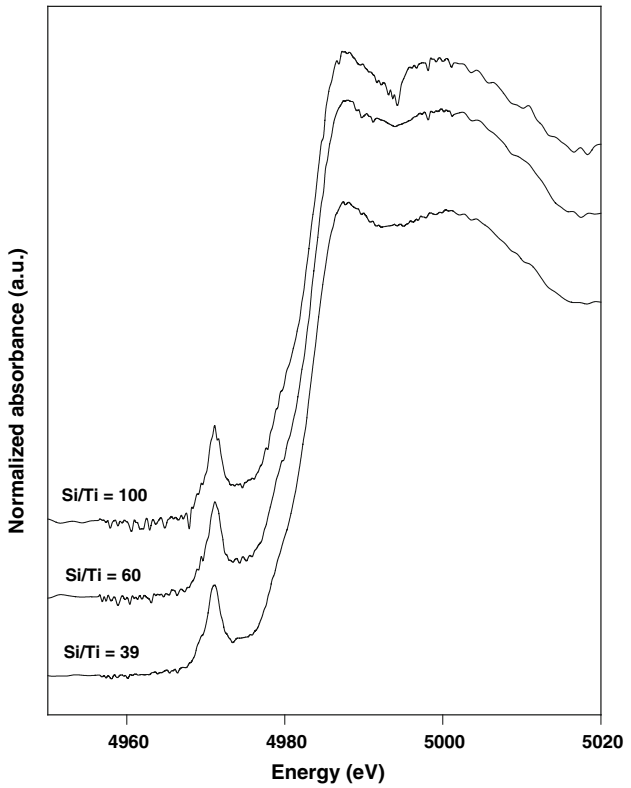

Fig. 4 Ti K-edge XANES spectra of Ti-MCM 41 with Si/Ti = 39–100

references is checked later independently by confirming that the sum of Ti–O–Ti and Ti–O–Si fractions makes unity. In the linear combination of XANES on our materials, the reference spectra were denoted as TOS and TOT for Ti–O–Si and Ti–O–Ti bonds in tetrahedral and octahedral symmetry, respectively.

Figure 5 shows the results of preedge fitting by the linear combination of two reference XANES over Ti-MCM 41 catalysts. In the Fig. 5, solid line indicates the experimental data, dotted line indicates the fit, while dashed line indicates the contribution from each reference spectrum. The numerical results of the fitting are summarized in Table 3. Two parameters χ_v^2 and *R-factor* related to the goodness of the fitting are defined as follows;

$$\chi_v^2 = \frac{1}{(N-P)\cdot\varepsilon^2}\sum_{i=1}^{N}\left(f_{\exp,i} - f_{model,i}\right)^2$$

$$R-factor = \frac{\sum_{i=1}^{N}\left(f_{\exp,i} - f_{model,i}\right)^2}{\sum_{i=1}^{N} f_{\exp,i}}$$

where f_{exp} is experimental data, f_{model} is an fitting function, N is the number of data points, P is the number of parameters in the fitting function, and ε is the uncertainty approximated by random fluctuation in the data. The fraction of TOT increases as Si/Ti ratio decreases while

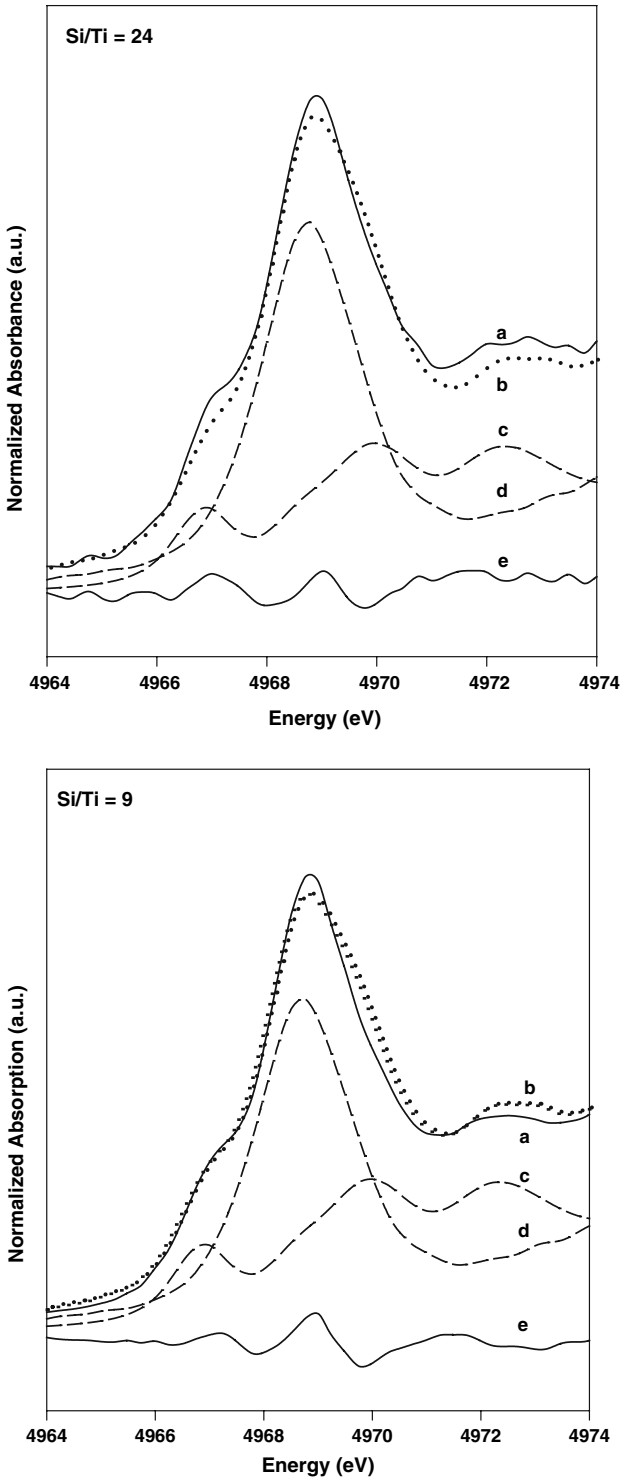

Fig. 5 Examples of Preedge fitting of XANES spectra of Ti-MCM 41 by linear combination of reference XANES spectra. Solid line is experimental spectrum in the preedge region and dotted line is the fitted result. Deconvoluted reference spectra is also included as dashed lines along with residual

Table 3 Pre-edge fitting parameters for Ti-MCM 41 catalysts

Si/Ti	c_{TOT}[a]	c_{TOS}[a]	ΔE_{TOT}[b]	ΔE_{TOS}[b]	χ_v^2 ($\times 10^{-5}$)[c]	R-factor ($\times 10^{-3}$)[d]
9	0.534	0.466	0.715	1.258	4.33	2.43
12	0.531	0.469	0.643	1.230	3.53	1.78
17	0.524	0.476	0.570	1.150	8.06	2.42
24	0.503	0.497	0.717	1.297	7.08	2.90

[a] Normalized concentration

[b] Energy shift correction, eV (±0.02 eV at maximum)

[c] Reduced χ^2

[d] R-factor

that of TOS decreases. The normalized concentration of TOS decreases from 0.497 to 0.466 over the range of prepared Si/Ti ratio, while TOT increased from 0.503 to 0.534.

4 Discussion

Transesterification of DMC and phenol to MPC was carried out over TiO_2/SiO_2 and Ti-MCM 41 catalysts. In case of TiO_2/SiO_2, silica supports with different pore sizes have been used. Titanium concentration was fixed at 10 wt% in all samples as we optimized this concentration in our previous report. As the pore size increases the surface area decreases as shown in Table 1. The total surface concentration of titanium was calculated from the multiplication of specific surface area (by BET) and titanium concentration atomic % (by XPS). Although the bulk atomic concentration of titanium in all catalysts is the same, the titanium surface area is different. In case of Davisil silica the TiO_2 surface area is high whereas in Q-series support it decreases as the pore size increases. We can observe from the Table 1, that as the TiO_2 surface area increases, the conversion of phenol increases, hence the yield of MPC also increases. These results prove that there is no effect of pore size on the activity of the catalysts. The catalytic activity solely depends upon the titanium surface area. Davisil silica shows the highest activity as the titanium surface area is the highest in this sample. From these results we can conclude that the reaction is not diffusion-limited but the surface reaction rate limiting and totally depend upon the titanium surface area.

Similar reaction has been carried out over Ti-MCM 41 catalysts. The results are shown in the Table 2. In this case also we observed the similar trend, Thus, BET surface area is almost the same but the titanium surface concentration (by XPS) is different (from 0.34 to 1.16) with different Si/Ti ratio, the phenol conversion is varied accordingly. As the Si/Ti ratio decreases, the titanium amount on the surface increases and hence the conversion of phenol increases. The Si/Ti = 9 shows highest conversion as this catalysts contains the highest amount of titanium on the surface. The conversion of phenol totally depends upon the titanium surface area. These results are consistent with the results observed from TiO_2/SiO_2 catalysts.

The structure of the catalysts was examined by XRD analysis. As shown in Fig. 1a, the broad peaks in the XRD patterns are indicative of the amorphous nature of the TiO_2/SiO_2 catalysts. The titanium in the catalysts exists as an anatase phase regardless of the nature of the silica support. However, in Ti-MCM-41 catalysts, as the concentration of titanium increases, the (100) peak shifts to a lower angle. It is important to note that Si/Ti ratio play a critical role in the formation of Ti-MCM-41 structure because representative peaks for that structure become highly diffused in the XRD pattern of the material with Si/Ti = 9, the highest Ti loading.

The coordination state of Ti in catalysts was revealed by Ti K-edge XANES for both TiO_2/SiO_2 and Ti-MCM 41. While titanium in TiO_2/SiO_2 possesses octahedral symmetry, Ti-MCM-41 contains tetrahedral Ti(IV) as well as octahedral Ti(IV). As the ratio of Si/Ti in Ti-MCM-41 decreases, the titanium concentration increases and hence the octahedral concentration increases. When the structure of Ti-MCM 41 is considered, only titanium atoms which are in the framework show the tetrahedral symmetry, whereas the Ti atoms which are out of the framework show the octahedral symmetry. We applied the linear combination procedure of Ti K-edge XANES [20–22] to quantify the TOT and TOS fractions in the Ti-MCM 41 samples. The fraction of TOT increases from 0.503 to 0.534 over Si/Ti = 24 to Si/Ti = 9 where as fraction of TOS decreases from 0.497 to 0.466. As the titanium concentration decreases, the formation of the framework Ti is favored. We further decreased the Ti concentration up to the Si/Ti = 100. As revealed in Fig. 4, the decrease of Ti below the ratio of Si/Ti = 24 would form octahedral holes, instead of increasing the amount of tetrahedral Ti. Therefore the Si/Ti = 24 is the saturation limit for titanium to be in the framework in this study. Below this ratio, Ti atoms out of framework gradually increases while the framework Ti decreases with increasing Ti loadings. Below the ratio Si/Ti = 9 the Ti-MCM 41 structure appears to collapse.

We correlated our linear combination data with the reaction results. Figure 6 displays both the results of XANES linear combination fitting and the conversion of phenol. The total titanium concentration is also included in the figure. The slope of the phenol conversion is similar to that of the total amount of titanium in the catalysts. The fraction of TOS and TOT does not seem to have any correlation with the conversion. As a result, turnover rate of MPC formation based on total titanium on the surface shows very little variation in the whole Si/Ti ratios as

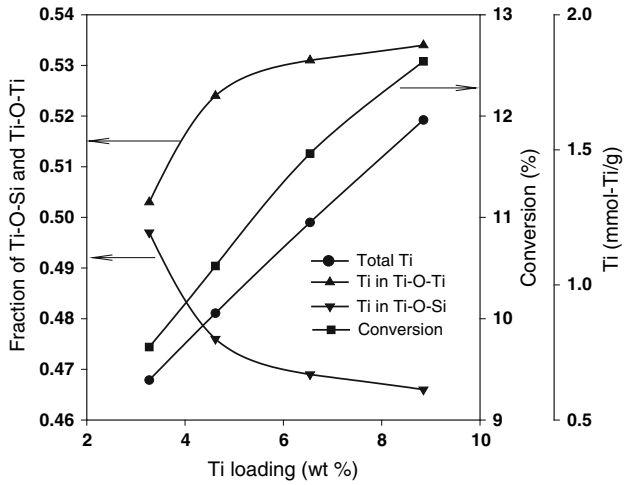

Fig. 6 Correlation between the fraction of Ti–O–Ti, Ti–O–Si and total Ti with phenol conversion for Ti-MCM 41 catalysts with different Si/Ti ratio

shown in Table 2. Therefore, it can be summarized that the phenol conversion depends upon the total titanium concentration, independent of the site symmetry of Ti in the catalysts.

Structure sensitivity of catalytic reactions is a convenient indication of the nature of the reaction. The turnover rates of MPC formation are independent of the titanium symmetry of tetrahedral or octahedral coordination with surrounding oxygen. Furthermore, those are also similar to those observed for TiO_2/SiO_2 catalysts of completely different structure. Hence, it could be concluded that transesterification of DMC over TiO_2/SiO_2 and Ti-MCM 41 is a structure insensitive reaction.

5 Conclusion

Silica supported titanium dioxide (TiO_2/SiO_2) and Ti-MCM 41 catalysts have been used for transesterification of dimethylcarbonate and phenol to methylphenylcarbonate. The structure and the chemical state of titanium species in TiO_2/SiO_2 and Ti-MCM 41 have been investigated by means of X-ray diffraction, Ti K-edge XANES, and XPS. To understand the role of pore size on the activity of catalysts, different pore size silica support (Q-series) was utilized. Similarly, to understand the Ti symmetry effect on the activity of catalysts, Ti-MCM 41 was used with different Ti-loading. It is observed that the Ti surface area is the only important factor to achieve highest activity. In case of Ti-MCM 41 catalysts, as the Ti-loading increases, octahedral symmetry increases and tetrahedral symmetry decreases. However, the turnover rates were independent of Ti-symmetry, but depended upon the total Ti-concentration on the surface of the catalysts. They are also similar to those for TiO_2/SiO_2 catalysts. Thus, it is concluded that the reaction is structure insensitive.

Acknowledgments We appreciate the support of the Korea Ministry of Education and Human Resources Development through the BK 21 program. Experiments at PAL were supported in part by MOST and POSTECH. UAJ thanks to Dr. Nark Eon Sung for helpful discussion.

References

1. Komiya K, Fukuoka S, Aminaka M, Hasegawa K, Hachiya H, Okamoto H, Watanabe T, Yoneda H, Fukawa I, Dozon T (1996) Green chemistry: designing chemistry for the environment. American Chemical Society, Washington DC. p 20
2. Chemistry in Britain (1994) 30:970
3. Gong J, Ma X, Wang S (2007) Appl Catal A 316:1
4. Kim WB, Joshi UA, Lee JS (2004) Ind Eng Chem Res 43:1897
5. Shaikh AG, Sivaram S (1996) Chem Rev 96:951
6. Song HY, Park ED, Lee JS (2000) J Mol Catal A 154:243
7. Fu Z-H, Ono Y (1997) J Mol Catal A 118:293
8. Cao M, Meng Y, Lu Y (2005) Catal Commun 6:802
9. Zhou WQ, Zhao XQ, Wang YJ, Zhang JY (2004) Appl Catal A 260:19
10. Mei FM, Pei Z, Li GX (2004) Org Process Res Dev 8:372
11. Fukuoka S, Deguchi R, Tojo M (1992) US Patent 5166393
12. Shaikh AG, Sivaram S (1992) Ind Eng Chem Res 31:1167
13. Lee H, Kim SJ, Ahn BS, Lee WK, Kim HS (2003) Catal Today 87:139
14. Kim WB, Lee JS (1999) Catal Lett 59:83
15. Kim WB, Lee JS (1999) J Catal 185:307
16. Kim WB, Kim YG, Lee JS (2000) Appl Catal A 194–195:403
17. Rhee CH, Lee JS (1997) Catal Today 38:213
18. Newville MJ (2001) J Synchrotron Rad 8:322
19. Bordiga S, Coluccia S, Lamberti C, Marchese L, Zecchina A, Boscherini F, Buffa F, Genoni F, Leofanti G, Petrini G, Vlaic G (1994) J Phys Chem 98:4125
20. Kim WB, Choi SH, Lee JS (2000) J Phys Chem B 104:8670
21. Kim WB, Choi SH, Lee JS (2001) J Phys Chem B 105:6274
22. Lee JS, Kim WB, Choi SH (2001) J Synchrotron Rad 8:163
23. Greegor RB, Lytle FW, Sandstrom DR, Wong J, Schultz P (1983) J Non-Cryst Sol 55:27
24. Sandstrom DR, Lytle FW, Wei PSP, Greegor RB, Wong J, Schultz P (1980) J Non-Cryst Sol 41:201